Reducing stochasticity in the North Atlantic Oscillation index with coupled Langevin equations

Pedro G. Lind,[1,2] Alejandro Mora,[3] Jason A. C. Gallas,[1,4] and Maria Haase[3]
[1]*Institute for Computational Physics, Universität Stuttgart, Pfaffenwaldring 27, D-70569 Stuttgart, Germany*
[2]*Centro de Física Teórica e Computacional, Av. Prof. Gama Pinto 2, 1649-003 Lisbon, Portugal*
[3]*Institut für Höchsleistungsrechnen, Universität Stuttgart, Nobelstr. 19, D-70569 Stuttgart, Germany*
[4]*Instituto de Física, Universidade Federal do Rio Grande do Sul, 91501-970 Porto Alegre, Brazil*
(Received 3 June 2005; published 11 November 2005)

We present a critical investigation of the functional relationship between the two pressure time series routinely used to define the index characterizing the North Atlantic Oscillation (NAO), well known to regulate global climate variability and change. First, by a standard Markov analysis we show that the standard NAO index based on the pressure difference is not optimal in the sense of producing sufficiently reliable forecasts because it contains a dominating stochastic term in the corresponding Langevin equation. Then, we introduce a variationally optimized Markov analysis involving two coupled Langevin equations tailored to produce a NAO quasi-index having the desired minimum possible stochasticity. The variationally optimized Markov analysis is very general and can be applied in other physical situations involving two or more time series.

DOI: 10.1103/PhysRevE.72.056706 PACS number(s): 02.50.Ga, 92.70.Gt

I. INTRODUCTION

The North Atlantic Oscillation (NAO) is increasingly becoming the focus of much attention in climate research lately because several studies show now its importance to rival with that of the El-Niño Southern Oscillation (ENSO) in terms of significance in global climate variability [1–7]. Together with ENSO, the NAO is a major source of seasonal to interdecadal variability in the global atmosphere [8,9]. Roughly speaking, the NAO describes a large-scale meridional vacillation in atmospheric mass between the anticyclone over Azores and the subpolar low pressure system over Iceland.

The spatial pattern of the NAO is a pronounced dipolelike pressure anomaly over the North Atlantic, with one pole at the Azores high and another over the Iceland low. This dipole has two main phases [8]: a positive NAO phase, when there is a strong pressure gradient between Iceland and Azores, and a negative phase, when the pressure gradient gets weaker. The positive NAO phase is associated, for instance, with stronger westerlies over the eastern North Atlantic and the European continent and with high precipitation over Scotland and Norway [4,8,10]. The negative phase is associated with weaker westerlies, with high precipitation over the Mediterranean and Black Sea, and with the surface air temperature in the North Atlantic [2,6,8,10]. Other variables, such as sea-ice levels and the geopotential heights, are also affected by the NAO phenomenon [3,4].

Traditionally, the state of the NAO dipole system is characterized by an index, the so-called NAO index $\mathcal{N}$, which is basically the pressure difference between the pressure P_1 at the high NAO pole and pressure P_2 at the low pole, namely

$$\mathcal{N} \equiv \mathcal{N}(m,y) = P_1^*(m,y) - P_2^*(m,y), \tag{1}$$

where $P_i^*(m,y) \equiv [P_i(m,y) - \langle P_i \rangle(m)]/\sigma_i(m)$ with m, y denoting month and year, respectively, $\langle P_i \rangle(m)$ representing the average of the pressure P_i at the mth month over some significant period of years, and σ_i being the corresponding standard deviation. The fact that there are many possible locations from where to select P_1 and P_2 results in many different NAO indices [8]. One of the most widely accepted index is that discussed by Hurrel [9], based on the standardized air-pressure difference [11] between Portugal (Lisbon), P_1, and Iceland (Stykkisholmur), P_2.

The question of whether or not the NAO is a chaotic or a stochastic process was recently addressed in the literature by Stephenson *et al.* [12]. Except for a few rare events, Collette and Ausloos [13] have subsequently found that all partial distribution functions of the NAO monthly index fluctuations have a form close to a Gaussian, indicating a lack of predictive power of the present index. However, we think that this pronounced stochasticity could originate from Eq. (1), i.e., from a nonoptimal choice of the mathematical representation of the index. Instead of using the pressure differences, we ask whether it would be possible to find a better functional relationship between the pressures allowing one to extract from the data a dynamical equation with stochastic terms not so dominant.

The goal of this paper is to propose a simple procedure to obtain a new index with reduced stochasticity. The key point is to directly use the two pressure time series and set up a variational problem allowing one to quench noise terms in an appropriate Langevin equation. Technically, this can be done as follows. Consider the normalized pressure series P_i^* as the dynamical variables of two coupled systems and for them to obtain a system of equations involving two coupled Langevin equations governing the evolution of the pressure increments. Next, transform variables, from pressures into two new variables, or "quasi-indices." Then, by imposing a minimum condition in one of the new variables one gets a variational problem which yields an optimal functional relationship between the pressures. The Langevin equation underlying this variationally optimized Markov analysis has the smallest stochastic terms.

The variationally optimized Markov analysis being introduced here may also be applied to generic situations involving two or more time series correlated (coupled) with each

other. In particular, the variational approach is expected to be useful in problems where the familiar Markov analysis of single time series has already proved to be efficient, for instance, to study small-scale turbulence [14], dynamical systems, such as the stochastic Lorenz system [15], statistics of the foreign exchange U.S. market [16], the roughness of surfaces [17], and also in the geophysical context, namely to study liquid water paths in clouds [17,18] and surface winds [19].

We start by reviewing briefly in Sec. II the general theory and numerical procedures to derive the Langevin equation from the time series and in Sec. III we apply these procedures to the monthly NAO index. Although in the case of the NAO index there is only a small amount of available measurements, the Markov analysis yields still reasonable results. We show that the Langevin equation underlying the evolution of NAO index increments as a function of delay times is highly stochastic, precluding its use for predictions. In Sec. IV we extend the Markov analysis to the pair of pressure time series from which the NAO index is usually calculated [9]. We find that the underlying system of two coupled Langevin equations still has high stochasticity. Finally, in Sec. V we introduce our main contribution, the variationally optimized Markov analysis, which allows us to obtain a new functional involving the pair of pressure measurements. For this functional the Langevin equation yields minimum stochasticity. Discussions and conclusion are given in Sec. VI.

II. MARKOV PROCESSES AND TIME SERIES

Friedrich, Peinke, and co-workers have recently shown [14–16,20] how to use experimental data to reconstruct the dynamics of a system presumed to underly a stochastic time series, under the assumption that the process is Markovian. Their numerical procedure for reconstruction is based on the derivation of drift and diffusion coefficients directly from measured data. From the first and second order conditional moments (of the conditional probability distribution of the index $\mathcal{N}$) one obtains Fokker-Planck and Langevin equations for the evolution of the system, whenever the fourth conditional moment of the increments vanishes [21]. In this section we describe briefly this procedure for a generic time series $\{X(n)\}$ where $n=1,\ldots,N$.

The starting point is the construction of auxiliary time series $\{X_{2t}(n)\}$, where $X_{2t}(n)=X(n+t)-X(n-t)$ for $n=t+1,\ldots,N-t$, where t is an integer. To each auxiliary time-series corresponds a probability density function $p(X,2t)$. The process is a Markovian one when the multiconditional probability density function (PDF) fulfills a Chapman-Kolmogorov equation [21]. If, in addition, the fourth conditional moment vanishes, then one can consider that there is a diffusion process over time increments underlying the time series, which can be described by a Fokker-Planck equation [21]. This diffusion process is governed by the Langevin equation

$$\frac{d}{d\tau}X_\tau = D^{(1)}(X_\tau,\tau) + \eta(\tau)\sqrt{D^{(2)}(X_\tau,\tau)}, \tag{2}$$

where $\eta(\tau)$ is a Langevin force (δ-correlated Gaussian noise), and $D^{(1)}$ and $D^{(2)}$ are the first two Kramers-Moyal coefficients, the drift and the diffusion coefficients, respectively, given by

$$D^{(k)}(X_\tau,\tau) = \frac{1}{k!}\lim_{\Delta\tau\to 0} M^{(k)}(X_\tau,\tau,\Delta\tau), \tag{3}$$

where $k=1,2$ and $M^{(k)}(X_\tau,\tau,\Delta\tau)$ are the conditional moments. These moments are given by

$$M^{(k)}(X_\tau,\tau,\Delta\tau) \simeq \frac{1}{\Delta\tau}\sum_{X_{\tau+\Delta\tau}} [X_{\tau+\Delta\tau}(n) - X_\tau(n)]^k p, \tag{4}$$

where the sum is taken over histograms of the PDFs of $X_{\tau+\Delta\tau}$ and $p\equiv p(X_{\tau+\Delta\tau},\tau+\Delta\tau|X_\tau,\tau)$ is the conditional probability given by the Bayes theorem, extracted directly from the auxiliary time series. A more detailed description of these procedures can be found in Ref. [14].

For practical purposes, the time t labeling the time series is rescaled in Eqs. (2)–(4), to $\tau=\log_2(\ell_M/t)$ where ℓ_M is the Markov length, i.e., a time lag beyond which the values of the time series are uncorrelated [16].

III. THE MONTHLY NAO INDEX AS A STOCHASTIC PROCESS

In this section we assume the monthly NAO index time series to be a Markovian process in time and perform the standard Markovian analysis [14–16]. As will become clear, such time series are highly stochastic, meaning that forecasts based on them are unreliable. Here we present a complete description of the main steps of the standard method, but also including error analysis.

Figure 1 shows the time series of the standard monthly NAO index between Portugal (Lisbon) and Iceland (Stykkisholmur) from January 1825 up to November 2002. Consecutive values in this series are highly uncorrelated as can be checked by evaluating the correlation function

$$C(t) = \frac{1}{(N-1)\sigma^2}\sum_{k=1}^{N}[\mathcal{N}(k+t)-\bar{\mathcal{N}}][\mathcal{N}(k)-\bar{\mathcal{N}}], \tag{5}$$

where $\bar{\mathcal{N}}$ is the index average and σ^2 the corresponding variance. When the system is nonlinear, one computes [22] the

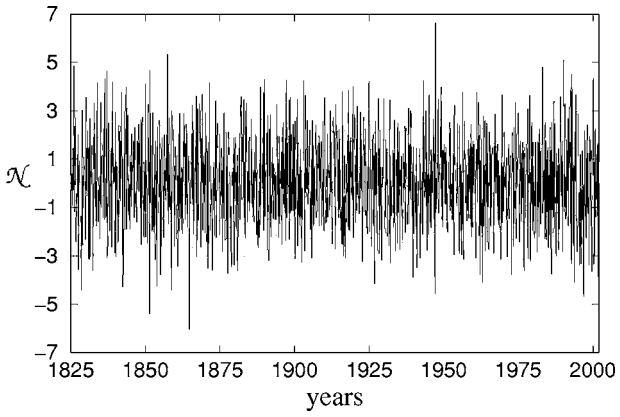

FIG. 1. Time series of the monthly NAO index $\mathcal{N}$ as defined in Eq. (1), computed from measured data [11].

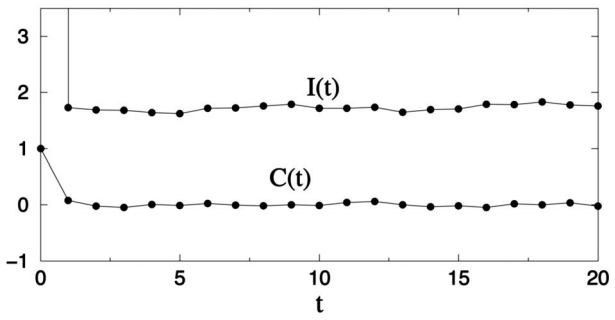

FIG. 2. The correlation function $C(t)$ and mutual information $I(t)$ for the standard monthly NAO index $\mathcal{N}$ as defined in Eq. (1). As one sees, correlations may be neglected for $t>1$ (see text).

mutual information $I(t)$ and records the first time that it decreases abruptly. As can be seen from Fig. 2 the correlation function $C(t)$ vanishes for $t\simeq 1$ month while the mutual information decreases abruptly for this same time lag. Thus, both quantities indicate that consecutive values of the NAO index are essentially uncorrelated. Nonlinear dependencies might still exist motivating a Markovian analysis as follows.

The conditional moments $M^{(1)}$ and $M^{(2)}$ defined in Eq. (4) are computed from the time series in Fig. 1 as a function of the time difference $\Delta t=t_{ref}-t$, where t_{ref} is the maximum value of t considered. Figure 3 shows $M^{(1)}(\mathcal{N}_{2t},t,\Delta t)$ and $M^{(2)}(\mathcal{N}_{2t},t,\Delta t)$ for $t_{ref}=32$ and $\mathcal{N}_{2t}(n)\equiv\mathcal{N}(n+t)-\mathcal{N}(n-t)$ at three different arguments of its PDF, namely, $\mathcal{N}_{2t}=\bar{\mathcal{N}},\bar{\mathcal{N}}+\sigma$ and $\bar{\mathcal{N}}-\sigma$. From a visual inspection one sees that for small Δt the conditional moments behave in an irregular fashion, while for $\Delta t\gtrsim 16$ they vary approximately linearly with the time lag. In fact, scaling arguments [13] indicate that a suitable choice for the Markov length is $\ell_M=16$ and we take this value as the Markov length for the time series, as indicated by the vertical dotted line. At the end of this section we confirm that this was indeed a proper choice. The error bars of the conditional moments are computed in the standard way (see Appendix A).

The limit in Eq. (3) is obtained using the rescaled time lag $\Delta\tau=\tau-\tau_{ref}=\log_2(t_{ref}/t)$, making a linear fit to $M^{(1)}$ and $M^{(2)}$ beyond the Markov length, and intersecting it with the vertical axis $\Delta\tau=0$. This limit gives an approximate value for the corresponding Kramers-Moyal coefficients, the drift $D^{(1)}$ and the diffusion $D^{(2)}$, respectively. Note that the horizontal axis in Fig. 3 is scaled with $\Delta t=t_{ref}-t$ to plot all points equally spaced. The limit $\Delta\tau\to 0$ implies $\Delta t\equiv t_{ref}-t\to 0$ since $\Delta\tau=\log_2(\ell_M/t)-\log_2(\ell_M/t_{ref})=\log_2(t_{ref}/t)$.

Fitting several values of $\mathcal{N}_\tau$ it is possible to compute both the drift $D^{(1)}$ and the diffusion $D^{(2)}$ coefficients as a function of $\mathcal{N}_\tau$, as illustrated in Fig. 4 for three references, namely $t_{ref}=32$, 64, and 96. The error bars of both Kramers-Moyal coefficients are determined directly from the linear fit algorithm [23], taking the values of the conditional moments and the corresponding errors as input. From Fig. 4 one clearly sees that the drift coefficient $D^{(1)}$ varies linearly with $\mathcal{N}_\tau$ while the diffusion coefficient $D^{(2)}$ varies quadratically. Further, one observes a slight asymmetry of the diffusion coefficient around $\mathcal{N}=0$. This asymmetry may be due to the different time intervals during which the NAO index spends in the positive and negative phase.

Taking $t_{ref}=32$ as a reference we find the parametrizations

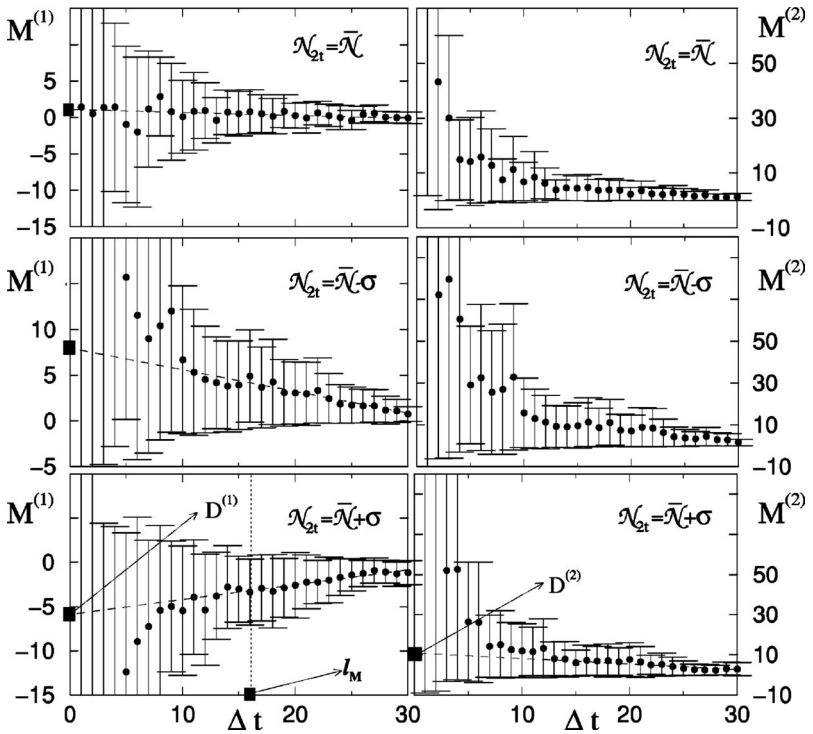

FIG. 3. The first and second conditional moments, $M^{(1)}$ and $M^{(2)}$ for the time series $\mathcal{N}$ shown in Fig. 1. Here $t_{ref}=32$ and $\mathcal{N}_{2t}=\bar{\mathcal{N}}$ (top), $\mathcal{N}_{2t}=\bar{\mathcal{N}}-\sigma$ (center), and $\mathcal{N}_{2t}=\bar{\mathcal{N}}+\sigma$ (bottom). Fitting the curves beyond the Markov length $\ell_M=16$ and intersecting the fits with the vertical axis $\Delta t=0$ yields the corresponding Kramers-Moyal coefficient (see text).

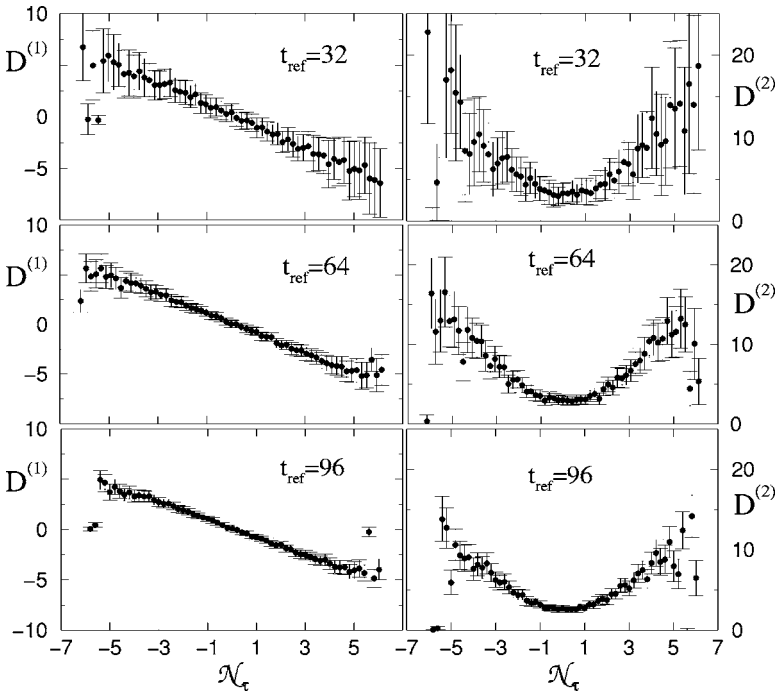

FIG. 4. The drift and diffusion coefficients, $D^{(1)}$ and $D^{(2)}$, obtained from linear fits of the corresponding conditional moments (see dashed lines in Fig. 3). Here $\mathcal{N}_\tau$ is given in the same units as the NAO index and varies within the range $[-6,6]$ for $t_{ref}=32$ (top), $t_{ref}=64$ (center), and $t_{ref}=96$ (bottom).

$$D^{(1)}(\mathcal{N}_\tau) = d_1^{(1)} + d_2^{(1)}\mathcal{N}_\tau, \tag{6}$$

$$D^{(2)}(\mathcal{N}_\tau) = d_1^{(2)} + d_2^{(2)}\mathcal{N}_\tau + d_3^{(2)}\mathcal{N}_\tau^2, \tag{7}$$

where

$$d_1^{(1)} = 0.150 \pm 0.013, \tag{8a}$$

$$d_2^{(1)} = -1.048 \pm 0.003, \tag{8b}$$

$$d_1^{(2)} = 3.47 \pm 0.05, \tag{8c}$$

$$d_2^{(2)} = -0.158 \pm 0.015, \tag{8d}$$

$$d_3^{(2)} = 0.407 \pm 0.003. \tag{8e}$$

These parametrizations do not completely agree with those found by Collette and Ausloos [13]. The difference is probably due to differences in the data sets used, since they consider the normalized pressures at different locations of both pressure subsystems, namely, P_1 is taken from Ponta Delgada (Azores) and P_2 from Akureyi (Iceland). Inspite of this, the main features agree well, since in both cases there is a negative slope in the drift coefficient, indicating a restoring force for the evolution of increments, as well as a quadratic dependence of the diffusion coefficient on the increments.

For other reference times, the parameterizations found are equal to Eqs. (6) and (7) within the error bars. Therefore, we may assume that both coefficients do not depend significantly on the reference time chosen.

The analysis performed in this section was made under the assumption that the process is Markovian, i.e., the conditional probability $p(\mathcal{N}_{\tau+\Delta\tau}, \tau+\Delta\tau|\mathcal{N}_\tau, \tau)$ constrained only to the previous time step equals the conditional probability $p(\mathcal{N}_{\tau+\Delta\tau}, \tau+\Delta\tau|\mathcal{N}_\tau, \tau; \mathcal{N}_{\tau-\Delta\tau}, \tau-\Delta\tau; \ldots)$ constrained to any number of previous time steps. A comparison of these conditional probabilities is, however, not recommended since we deal with very small data sets ($\sim 2\times 10^3$ data points). Instead of providing evidence for coinciding conditional probabilities, we use the Kramers-Moyal coefficients in Eqs. (6) and (7) derived empirically and integrate the Fokker-Planck equation (B1) as described in Appendix B.

Figure 5 shows consecutive PDFs for $\Delta\tau=\log_2(t_{ref}/t)=0$, 1, 2, 3, and 4, corresponding to $t=32$, 16, 8, 4, and 2, respectively, starting from an initial PDF taken at $t_{ref}=32$. By integrating the Fokker-Planck equation, using the coefficients in Eqs. (8), one tests the validity of our approach, which assumes from the very beginning that the process is Markovian within a certain range of $\mathcal{N}$ increments, with a Markov length $\ell_M=16$. Notice that the noise level might be underestimated since we did not consider the errors of the NAO index measurements. Therefore, to improve the fits in Fig. 5 we used a larger value for $d_1^{(2)}$, keeping all the other coefficients as given in (8).

As one clearly sees from Fig. 5, the initial distribution retains its Gaussian shape through time and the PDFs of the data (indicated by circles) are well fitted by the PDFs obtained from the integration of the Fokker-Planck equation (solid lines) within the range $\mathcal{N}_\tau \in [-2,2]$. Thus, the Markov length $\ell_M=16$ chosen as well as the parametrization of the Kramers-Moyal coefficients in Eqs. (6) and (7) seem to be appropriate for the present situation.

From the results in this section one concludes that the standard NAO index $\mathcal{N}$ can be assumed as a stochastic process within the range $[-2,2]$, which corresponds approximately to one standard deviation of the PDF of the original $\mathcal{N}$ values plotted in Fig. 1. The fact that the Gaussian shape is almost invariant for any time lag means that the time series is highly stochastic and that the forecast based on them is unreliable. This conclusion agrees with results of Collette and Ausloos [13]. Here, however, a detailed error analysis

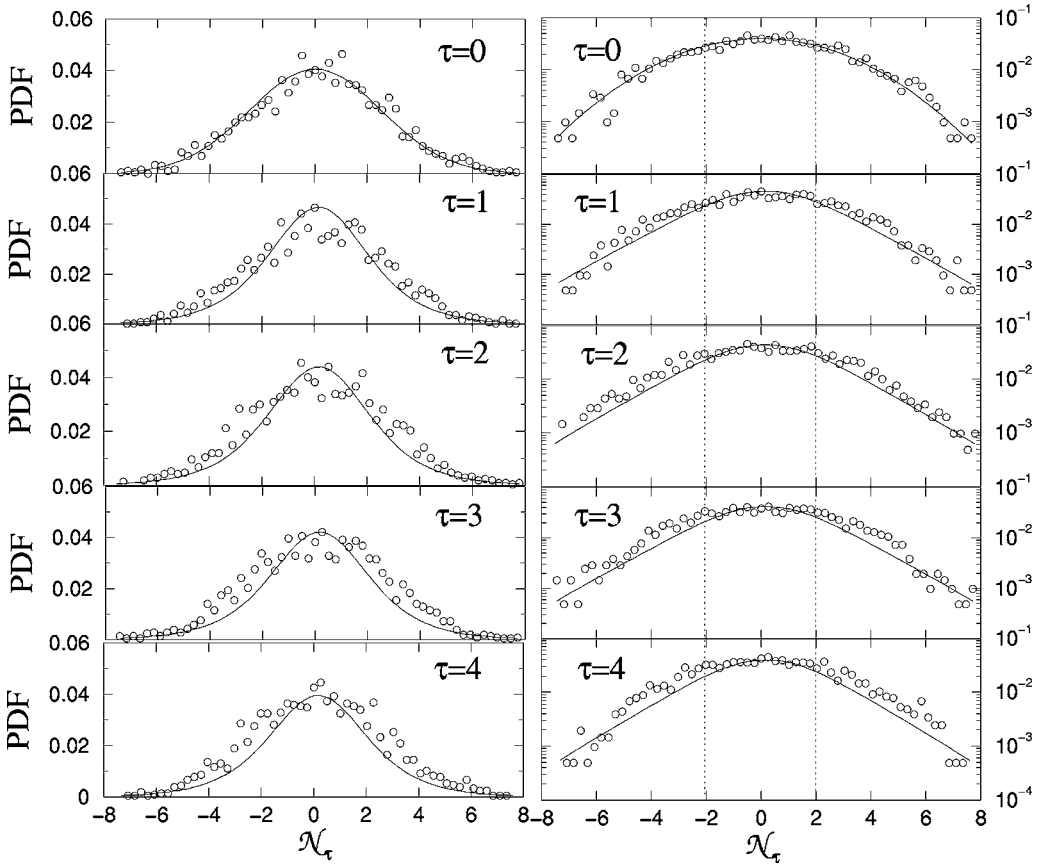

FIG. 5. Comparison between the probability density functions of the auxiliary time series for NAO (circles) and the integration of the Fokker-Planck equation (solid lines), starting with an initial PDF at $t_{ref}=32$. The integration begins at $t=t_{ref}$ ($\Delta\tau=0$) and PDFs are plotted at time steps $t=32,16,8,4,2$, i.e., at $\Delta\tau=\log_2(t_{ref}/t)=0,1,2,3,4$, respectively. For each time step the PDF is plotted in linear (left) and logarithmic (right) scales. The good agreement seen indicates the Markov length $\ell_M=16$ used in the simulation to be a good choice and the process to be almost Gaussian in the range $[-2,2]$ (see text).

was added, indicating the errors of all calculations, in particular, the ones of the parametrized coefficients in Eqs. (6) and (7). In the next sections we investigate the origin of the stochasticity and a way of minimizing it.

IV. COUPLED LANGEVIN EQUATIONS FOR THE NAO

As shown in the previous section, the NAO index leads to a highly stochastic time series with consequent lack of predictability. However, since the NAO index is a specific functional of the difference of the normalized pressures in the two poles, it seems natural to ask: Is it possible to find an alternative functional of the normalized pressures having smaller stochastic terms? In other words, is it possible to define a better index in the sense that it improves predictability? In the remainder of the paper we answer this question affirmatively. Instead of the standard NAO index, we work directly with both pressure series. First, in this section, we extend the Markov analysis by considering the two series as a coupled system. Then, in the next section, we describe how to obtain a better index for the NAO.

As mentioned, we now introduce a system of two coupled Langevin equations:

$$\frac{dP_1^*}{d\tau} = h_1 + g_{11}\eta_1(\tau) + g_{12}\eta_2(\tau), \tag{9a}$$

$$\frac{dP_2^*}{d\tau} = h_2 + g_{21}\eta_1(\tau) + g_{22}\eta_2(\tau), \tag{9b}$$

where P_i^* represents the normalized pressures, i.e., $P_i^*=(P_i-\langle P_i\rangle)/\sigma_i$ and, for simplicity, from now on we write P_i to represent these normalized pressures. Here, both η_1 and η_2 are also Langevin forces describing Gaussian noises with δ correlations, i.e., for $i=1,2$ one has $\langle\eta_i(\tau)\rangle=0$ and $\langle\eta_i(\tau)\eta_i(\tau')\rangle=\delta(\tau-\tau')$. The functions h_i and g_{ij}, where $i,j=1,2$ depend, in general, on P_1 and P_2 and τ and are given by [21]

$$h_i = D_i^{(1)}, \tag{10a}$$

$$g_{ij} = (\sqrt{D^{(2)}})_{ij}, \tag{10b}$$

where $D^{(1)}$ is the drift "vector" and $D^{(2)}$ the symmetrical diffusion matrix.

The procedure to compute drift and diffusion coefficients in two dimensions is a straightforward generalization of the one-dimensional case, as described in Appendix C. The re-

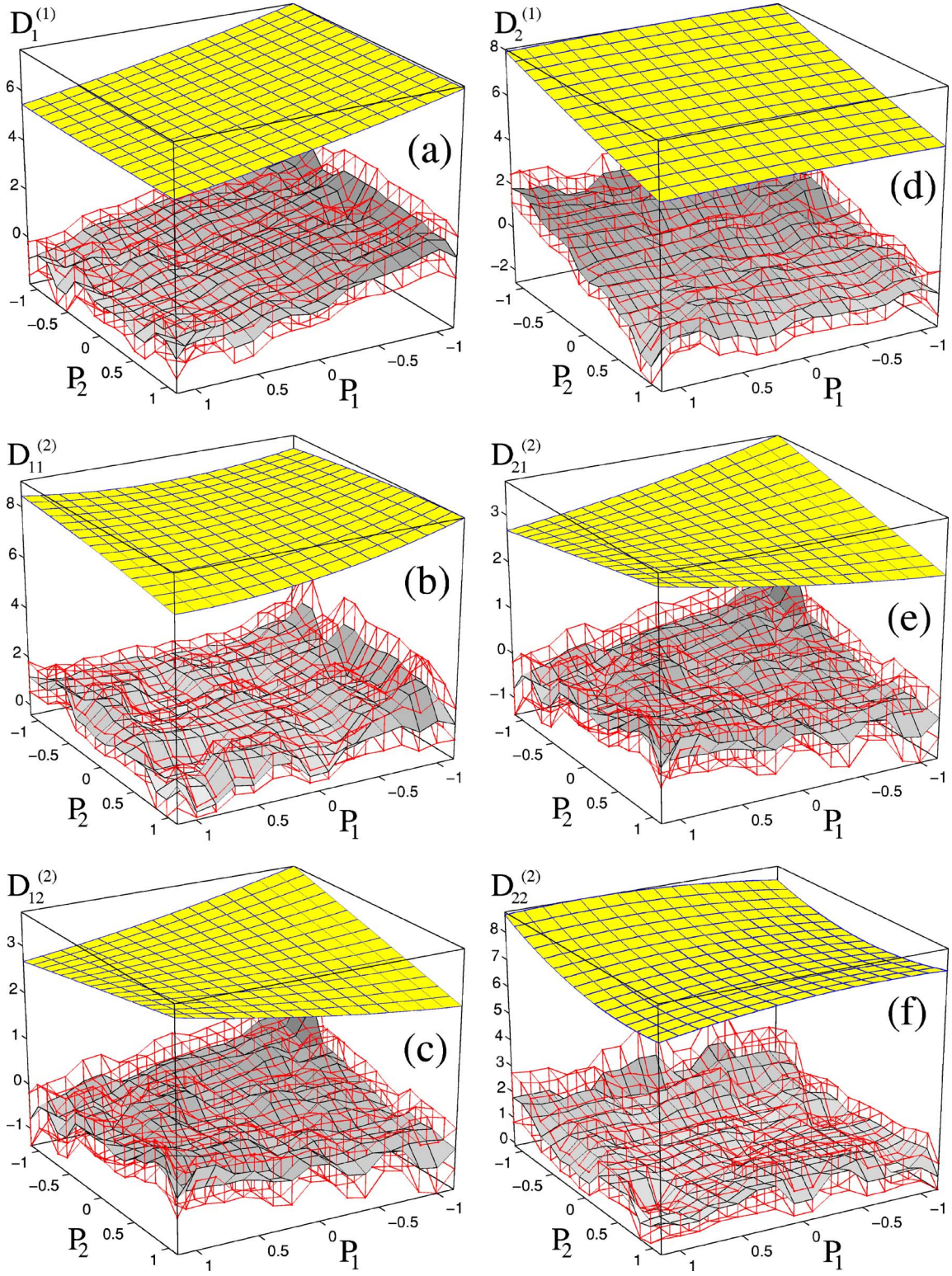

FIG. 6. (Color online) The Kramers-Moyal coefficients for the two coupled Langevin equations in (9): (a) $D_1^{(1)}$, (b) $D_{11}^{(2)}$, (c) $D_{12}^{(2)}$, (d) $D_2^{(1)}$, (e) $D_{21}^{(2)}$, and (f) $D_{22}^{(2)}$. Each plot shows a surface obtained from Eqs. (C1) in Appendix C and the corresponding fitted surface shifted for better inspection.

sult of these computations are surfaces in the $P_1 \times P_2$ plane. As for the standard index, our simulations have shown that the dependence on τ can be neglected here. Figure 6 shows these surfaces for all the Kramers-Moyal coefficients with the corresponding error bar at each grid point. At the bottom of each figure one sees the surfaces obtained from the data, while at the top the corresponding fitted surface is plotted. All fitted surfaces in Fig. 6 are quadratic forms

TABLE I. Parametrization coefficients of the drift vector $D^{(1)}$, diffusion matrix $D^{(2)}$, and of the functions g_{ij}. Due to symmetry $D_{21}^{(2)}=D_{12}^{(2)}$ and $g_{21}=g_{12}$. From Eq. (10) one also has $h_i=D_i^{(1)}$.

	α_1	α_2	α_3	α_4	α_5	α_6
$D_1^{(1)}$	−0.920	0.085	−0.007	0.036	0.026	0.220
	±0.062	±0.096	±0.058	±0.093	±0.089	±0.073
$D_2^{(1)}$	0.000	−0.048	−1.093	0.040	0.032	0.342
	±0.058	±0.092	±0.063	±0.099	±0.090	±0.072
$D_{11}^{(2)}$	−0.337	0.321	−0.089	−0.083	−0.280	0.818
	±0.054	±0.082	±0.047	±0.070	±0.074	±0.057
$D_{22}^{(2)}$	−0.028	−0.209	−0.323	0.425	−0.186	0.870
	±0.046	±0.073	±0.057	±0.087	±0.074	±0.059
$D_{12}^{(2)}$	−0.031	0.067	−0.091	−0.006	0.376	−0.184
	±0.034	±0.054	±0.037	±0.058	±0.053	±0.041
g_{11}	−0.171	0.143	−0.065	−0.063	−0.147	0.906
	±0.009	±0.014	±0.009	±0.015	±0.013	±0.012
g_{22}	−0.021	−0.119	−0.161	0.193	−0.089	0.931
	±0.009	±0.014	±0.009	±0.015	±0.013	±0.012
g_{12}	−0.014	0.047	−0.046	0.009	0.181	−0.106
	±0.009	±0.014	±0.009	±0.015	±0.013	±0.012

$$\mathcal{S}(P_1,P_2)=\alpha_1P_1+\alpha_2P_1^2+\alpha_3P_2+\alpha_4P_2^2+\alpha_5P_1P_2+\alpha_6. \tag{11}$$

Table I gives the coefficients α_i for both the drift vector $D^{(1)}$ and the diffusion matrix $D^{(2)}$ and also for the functions h_i and g_{ij} defined in Eq. (10).

From Table I one sees that the drift coefficients $D_1^{(1)}$ and $D_2^{(1)}$ are approximately linear, i.e., apart from the independent term, their dominant terms are P_1 and P_2, respectively. With this and from h_i, Eq. (10a), we can say that the deterministic parts of the Langevin equations (9) are almost uncoupled. In fact, the absence of coupling between the two deterministic parts is not surprising since we are considering "instantaneous" coupling and, since both pressure subsystems are distant from each other, any eventual influence of one subsystem on the other should be characterized by some delay time, large enough to enable propagation of information.

As for the diffusion matrix, the two main diagonal elements $D_{11}^{(2)}$ and $D_{22}^{(2)}$ have significant contributions from the quadratic terms. The same is true for the corresponding functions g_{11} and g_{22}. Curiously, there is a fundamental difference: while in g_{11} the quadratic term in P_1^2 is much higher than the one in P_2^2, in function g_{22} both quadratic terms have similar contributions. Thus, one could argue that the normalized pressure P_1 at the Azores high contributes more strongly to the stochastic evolution of the pressure P_2, than vice versa. In other words, there is a sort of unidirectional coupling of the stochastic forces between both subsystems, with P_2 more strongly coupled to P_1 than P_1 to P_2. This is analogous to recent results [24] indicating that P_1 has a stronger influence than P_2.

The off-diagonal terms $D_{12}^{(2)}=D_{21}^{(2)}$ and $g_{12}=g_{21}$, respectively, are dominated by P_1P_2 and, therefore, govern the symmetrical part of the coupling between both subsystems. The symmetric part of the coupling is due to the symmetry of the diffusion matrix: $D_{12}^{(2)}=D_{21}^{(2)}$ (see Appendix C).

Similar surfaces (not shown here) were obtained for h_i and g_{ij} in Eq. (9). The functions h_i are identical to the drift coefficient $D_i^{(1)}$ [Eq. (10a)]. To determine functions g_{ij} one must compute for each grid point a diffusion matrix and obtain its "square root" $\sqrt{D^{(2)}}$ [Eq. (10b)]. The matrix $\sqrt{D^{(2)}}$ is obtained from $D^{(2)}$ by imposing an orthogonal transformation which diagonalizes $D^{(2)}$, taking the positive square root of the eigenvalues along the main diagonal and applying the inverse of the orthogonal transformation [21]. Note that for any pair (P_1,P_2) the diffusion matrix is positive definite and, therefore, its eigenvalues are always positive, the corresponding square roots being real. Moreover, the same symmetry of the diffusion matrix yields $g_{ij}=g_{ji}$.

From the results in this section one sees that, as for the analysis based on a single Langevin equation, coupled Langevin equations still have high stochastic terms, in the sense that they contribute significantly to the evolution of the pressure variables. In the next section we show how to reduce this stochasticity to a minimum.

V. REDUCING STOCHASTICITY VARIATIONALLY

The purpose of this section is to introduce a general variational procedure allowing one to extract an optimal function of the two pressure variables yielding a Langevin equation with minimum stochasticity. As far as we know, this approach to reduce stochasticity is original. It can be applied to spatially extended (coupled) systems characterized by several time series correlated (coupled) with each other.

We start by considering the two coupled Langevin equations (9) whose coefficients h_i and g_{ij} are given in Table I.

From Eqs. (9), one can make a general transformation of variables $(P_1,P_2)\rightarrow(N_1,N_2)$ leading to a new system of equations

$$\frac{dN_1}{d\tau} = h_1' + g_{11}'\eta_1(\tau) + g_{12}'\eta_2(\tau), \tag{12a}$$

$$\frac{dN_2}{d\tau} = h_2' + g_{21}'\eta_1(\tau) + g_{22}'\eta_2(\tau), \tag{12b}$$

where the new coefficients are

$$h_i' = h_1\frac{\partial N_i}{\partial P_1} + h_2\frac{\partial N_i}{\partial P_2}, \tag{13a}$$

$$g_{ij}' = g_{1j}\frac{\partial N_i}{\partial P_1} + g_{2j}\frac{\partial N_i}{\partial P_2}, \tag{13b}$$

for $i,j=1,2$ and where the dependence on τ is neglected, since this is what happens for our time series, as shown in the previous section. One possible transformation of variables would be $N_1=P_1-P_2$ and $N_2=P_1+P_2$, which yields N_1 as the standard NAO index with strong stochasticity. Since, in general, the Jacobian of (13) does not vanish, many other choices are possible and the question we address now is for which choice are the stochastic terms minimal? To this end, we require that for one of the equations in (12), say Eq. (12a), both stochastic terms be as small as possible when compared to the deterministic one. In other words, the dependence of N_1 on P_1 and P_2 is such that a functional is minimized. We assume this functional to be

$$F = \frac{\|g_{11}'\|_{L_2}^2 + \|g_{12}'\|_{L_2}^2}{\|h_1'\|_{L_2}^2}, \tag{14}$$

where $\|f(P_1,P_2)\|_{L_2}$ is the L_2-norm of $f(P_1,P_2)$:

$$\|f(P_1,P_2)\|_{L_2} = \left(\int\int_{\Omega} |f(P_1,P_2)|^2 dP_1 dP_2\right)^{1/2}. \tag{15}$$

As will be seen below, in practice, it is only necessary to take a finite interval for the integration in both variables, typically $\Omega=[-1,1]\times[-1,1]$.

Without any additional condition it is difficult to minimize F in Eq. (14) since it is a quotient of integrals. Therefore we impose the additional constraint

$$\int\int_{\Omega} \frac{|h_1'|^2}{a} dP_1 dP_2 = 1, \tag{16}$$

where a is a suitable constant to be chosen in the next paragraph. Note that, since the constraint in Eq. (16) only imposes a value for the deterministic part of the evolution and the proposed variational method deals with the problem of minimizing stochastic terms when compared with deterministic ones, there are no spurious implications related with this condition.

The above considerations lead to a variational problem in two variables where one seeks to minimize F under the constraint (16). This produces the Lagrangian

$$L = (g_{11}')^2 + (g_{12}')^2 + \lambda\left[\frac{(h_1')^2}{a} - 1\right], \tag{17}$$

where λ is the Lagrangian multiplier. Since we are still free to chose a, without loss of generality we fix $a=\lambda$. This choice is equivalent to writing the functions h_1', g_{11}', and g_{12}' in Eq. (12a) in units of the L_2 norm of the deterministic function h_1'.

Substituting Eqs. (13) into Eq. (17), inserting the Lagrangian into the Euler-Lagrange equation

$$\frac{\partial L}{\partial t} - \frac{\partial}{\partial P_1}\left(\frac{\partial L}{\partial\left(\frac{\partial N_1}{\partial P_1}\right)}\right) - \frac{\partial}{\partial P_2}\left(\frac{\partial L}{\partial\left(\frac{\partial N_1}{\partial P_2}\right)}\right) = 0, \tag{18}$$

and with elementary manipulation we arrive to the equation

$$\mathcal{A}\frac{\partial N_1}{\partial P_1} + \mathcal{B}\frac{\partial N_1}{\partial P_2} + \mathcal{C}\frac{\partial^2 N_1}{\partial P_1^2} + \mathcal{D}\frac{\partial^2 N_1}{\partial P_2^2} + \mathcal{E}\frac{\partial^2 N_1}{\partial P_1 \partial P_2} = \mathcal{F}, \tag{19}$$

where

$$\mathcal{A} = \frac{\partial}{\partial P_1}(g_{11}^2 + g_{12}^2 + h_1^2) + \frac{\partial}{\partial P_2}(g_{11}g_{21} + g_{12}g_{22} + h_1h_2), \tag{20a}$$

$$\mathcal{B} = \frac{\partial}{\partial P_2}(g_{21}^2 + g_{22}^2 + h_2^2) + \frac{\partial}{\partial P_1}(g_{11}g_{21} + g_{12}g_{22} + h_1h_2) \tag{20b}$$

$$\mathcal{C} = g_{11}^2 + g_{12}^2 + h_1^2, \tag{20c}$$

$$\mathcal{D} = g_{21}^2 + g_{22}^2 + h_2^2, \tag{20d}$$

$$\mathcal{E} = 2(g_{11}g_{21} + g_{12}g_{22} + h_1h_2), \tag{20e}$$

$$\mathcal{F} = -\left(\frac{\partial h_1}{\partial P_1} + \frac{\partial h_2}{\partial P_2}\right). \tag{20f}$$

From the coefficients h_i and g_{ij} in Table I one sees that all coefficients in (20) are polynomials. More precisely, $\mathcal{A}$ and $\mathcal{B}$ are cubics, $\mathcal{C}$, $\mathcal{D}$, and $\mathcal{E}$ are quartics while $\mathcal{F}$ is a linear polynomial.

In the range Ω considered, the discriminant $(\mathcal{E}/2)^2-\mathcal{C}\mathcal{D}$ is always negative, indicating that Eq. (19) is an elliptic equation [25]. Substituting the standard index $N_1=P_1-P_2$ in Eq. (19) yields $\mathcal{A}-\mathcal{B}=\mathcal{F}$, a condition not holding for most values of P_1 and P_2, as is illustrated in Fig. 7. This fact demonstrates an important fact, namely, that the standard NAO index does not minimize the functional in Eq. (14) and, therefore, is not the function of P_1 and P_2 with minimal stochasticity.

Discretizing Eq. (19) suitably one obtains N_1 as a function of the previous variables P_1 and P_2, satisfying the variational problem in Eq. (14). In other words, one obtains a new functional $N_1\equiv N_1(P_1,P_2)$ such that its corresponding Langevin equation, Eq. (12a), has minimal stochasticity, as desired. Therefore, the new functional N_1 is a better NAO index in

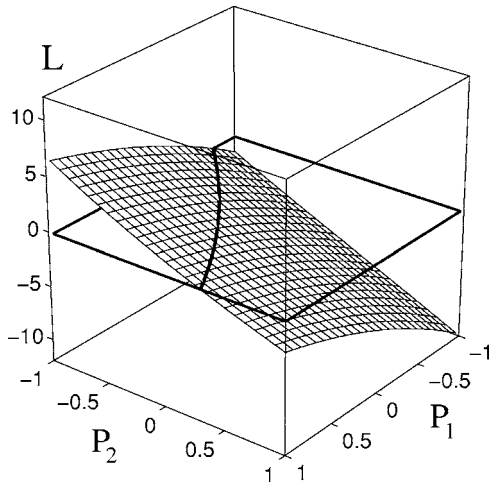

FIG. 7. Function $L=\mathcal{A}-\mathcal{B}-\mathcal{F}$ [see Eqs. (20)] as a function of P_1 and P_2 in the range $[-1,1]\times[-1,1]$. The contour line indicates $L=0$ for which Eq. (19) holds. Anywhere else the differential equation is not satisfied, meaning that the standard NAO index is not the one with minimal stochasticity (see text).

the sense that it enables more accurate forecasting, i.e., with less stochasticity, of the NAO system, extracted directly from the two measured pressure series. Similarly to the standard NAO index, forecasting of the pressure time series is still difficult and out from the scope of the present method. However, from the new index one can extract relevant physical information concerning the NAO system, for instance, an asymmetry in the coupling between both pressure subsystems, as we explain next.

To integrate Eq. (19) we suppose that at the boundaries N_1 is a linear function of either P_1 or P_2, while at the corners of $\partial\Omega$ one assumes $N_1=0$ at $(P_1,P_2)=(-1,-1)$ and $(P_1,P_2)=(1,1)$, $N_1=1$ at $(P_1,P_2)=(1,-1)$ and $N_1=-1$ at $(P_1,P_2)=(-1,1)$. This choice of boundary conditions is motivated by climatological facts concerning the NAO system. Namely, as mentioned in the Introduction, when P_1 is large and P_2 is small, the NAO system is in the positive phase, corresponding to high values of the index. Inversely, when P_1 is small and P_2 is large the index should be small. Thus, we assume that the index N_1 is maximal when P_1 is maximal and P_2 is minimal, and it is minimal when the opposite occurs.

Using centered differences to discretize derivatives in Eq. (19) and applying a successive over-relaxation algorithm [23] starting from the boundary conditions given in the last paragraph, one obtains the optimal N_1 as a function of P_1 and P_2. Figure 8 shows the surface $N_1(P_1,P_2)$ obtained in this way, where one clearly sees a deviation from a plane, meaning that N_1 is not linear in P_1 and P_2 as the standard index presupposes. The best least-square fit for this surface is also a quadratic form

$$N_1(P_1,P_2) = \beta_1 P_1 + \beta_2 P_1^2 + \beta_3 P_2 + \beta_4 P_2^2 + \beta_5 P_1 P_2 + \beta_6. \tag{21}$$

with

$$\beta_1 = 0.5407 \pm 0.0071, \tag{22a}$$

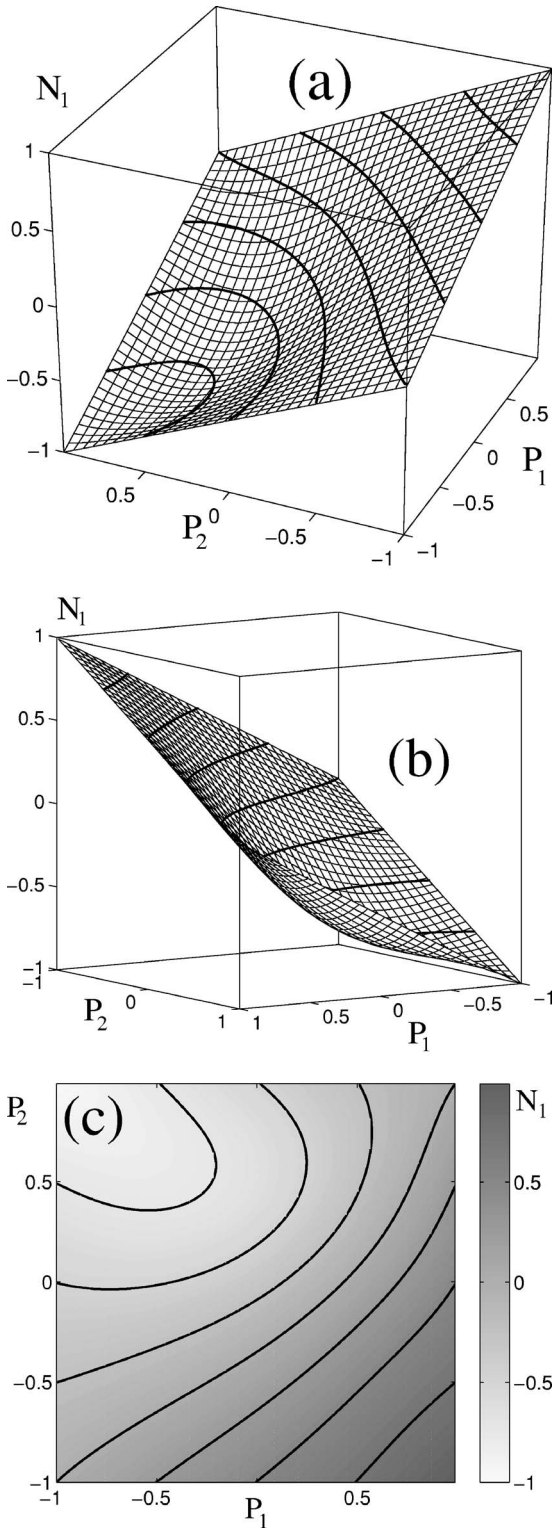

FIG. 8. Solution $N_1(P_1,P_2)$ of Eq. (19) with linear boundary conditions (see text), minimizing the variational in Eq. (14). In (a) and (b) the surface is shown in two different views, to emphasize its curvature, showing that N_1 is not linear in P_1 and P_2 as the standard NAO index. In (c) one sees the surface projected in the (P_1,P_2) plane with contour lines, emphasizing the asymmetry around the secondary diagonal $P_1=-P_2$.

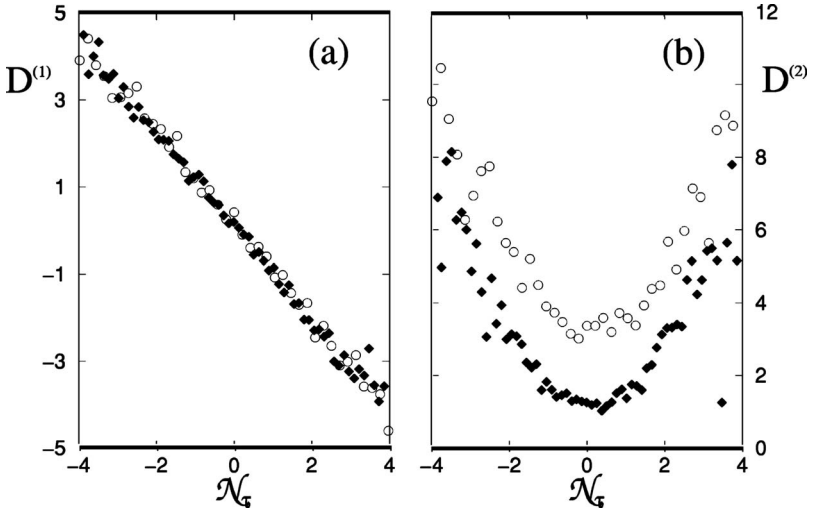

FIG. 9. Kramers-Moyal coefficients, as a function of the NAO index, for the optimized index (diamonds) compared with the standard index (circles): (a) Drift coefficient $D^{(1)}$ and (b) diffusion coefficient $D^{(2)}$. Here, the reference is $t_{ref}=32$.

$$\beta_2 = 0.2465 \pm 0.0122, \tag{22b}$$

$$\beta_3 = -0.6344 \pm 0.0006, \tag{22c}$$

$$\beta_4 = 0.3370 \pm 0.0011, \tag{22d}$$

$$\beta_5 = -0.0170 \pm 0.0122, \tag{22e}$$

$$\beta_6 = -0.3384 \pm 0.0005. \tag{22f}$$

While Figs. 8(a) and 8(b) emphasize the curvature of the surface $N_1(P_1,P_2)$, Fig. 8(c) shows the contour lines of the surface projected in the (P_1,P_2) plane. From this contour lines one clearly sees that there is an asymmetry due to the different coefficients of the terms in P_1 and P_2.

While the new index defined above has a time series which looks like that in Fig. 1 and has a correlation length slightly larger than the standard index, the diffusion coefficient decreases significantly. In fact, as illustrated in Fig. 9, while the deterministic part remains almost the same [see Fig. 9(a)] the stochastic term controlled by the diffusion coefficient decreases to approximately one-third of the coefficient for the standard index. More precisely, repeating the same Markov analysis as in Sec. III this time for the new index, one obtains a fit for the drift and diffusion coefficients of the form of Eqs. (6) and (7), respectively, with the parametrization

$$d_1^{(1),new} = 0.120 \pm 0.010, \tag{23a}$$

$$d_2^{(1),new} = -1.074 \pm 0.006, \tag{23b}$$

$$d_1^{(2),new} = 1.22 \pm 0.02, \tag{23c}$$

$$d_2^{(2),new} = -0.10 \pm 0.01, \tag{23d}$$

$$d_3^{(2),new} = 0.414 \pm 0.003. \tag{23e}$$

By comparing Eqs. (23) with the previous Eqs. (8), one sees that, while the parametrization for the drift coefficient (deterministic term) remains approximately the same, the diffusion coefficient ruling the stochasticity of the dynamics is now much smaller. In particular, $d_1^{(2),new} \sim d_1^{(2)}/3$.

VI. DISCUSSION AND CONCLUSIONS

In this paper we performed a detailed Markov analysis of the standard monthly NAO index comparing it with a more general analysis where, instead of the index derived from the pressure time series, we work with the measured pressures directly. In both situations we find stochastic terms to be large implying unreliable forecasting.

In order to reduce stochasticity we propose a general variational procedure which transforms variables from the two pressure time series into a pair of new variables, one of them having the minimum stochasticity possible. This variationally optimized Markov analysis is general and may be applied also to other systems characterized by two or more time series, correlated (coupled) with each other, for instance, in spatially extended systems. We believe that the variationally optimized Markov analysis represents a new development in the field. It should be helpful to deal with problems where the familiar Markov analysis of single time series has already proved to be efficient.

To delimit the validity of the variationally optimized Markov analysis one could check deterministic models, e.g., Lorenz system, introducing noise as an additional term, and try to obtain the optimal variable transformation from time series extracted from the system. This test will be reported elsewhere.

Concerning the particular case of the NAO system, although time series are relatively small (2135 points), yielding large errors, the results above gave evidence that the NAO index may be interpreted as a Markovian process and, with the variational problem proposed above, it was possible to obtain a functional relationship between both pressures having less stochasticity than the standard index. To use this new index for climatological purposes it would be necessary to redefine the two different phases of the NAO, in order to understand the physical meaning of it.

The correlation length of the present time series is small, due to the large time lag (one month) between consecutive

values of the time series. One possible way to further strengthen the role of the deterministic part in the NAO system is to consider shorter time lags. Although climatologists usually compute the standard NAO index between time intervals of one month or one year [8], since the last 50 years, the daily pressure of the two NAO subsystems was also recorded, enabling a standard definition of *daily* index similar to Eq. (1), with a much larger correlation length and a larger number of points. Preliminary results concerning the variational Markov analysis of this daily measures indicate that also in that case an optimized functional relationship is obtained, with less stochasticity than the standard daily NAO index. Moreover, by using time lags of one day instead of one month or one year, one could ascertain which time lag between, say one day and one month, gives better results for forecasting. From the Markov analysis it is also possible to ascertain which kind of noise, additive or multiplicative, the system has [26]. Finally, this approach could be extended by considering the impact of a delayed coupling, since the two subsystems composing the NAO system force one another within a certain time scale. The study of these questions and their relevance for climatological purposes are now being carried out and will be presented elsewhere [27].

ACKNOWLEDGMENTS

The authors thank Rudolf Friedrich, Joachim Peinke, and Rudolf Hilfer for useful remarks and discussions. P.G.L. thanks Fundação para a Ciência e a Tecnologia (FCT), Portugal, for financial support. J.A.C.G. thanks the Sonderforschungsbereich 404 of the DFG, Germany, and CNPq, Brazil for financial support.

APPENDIX A: ERROR ANALYSIS

The error bars in Figs. 3 are obtained from standard error analysis, namely the error, function for the conditional moments $M^{(k)}$ with $k=1,2$ read

$$\Delta M^{(k)}(\mathcal{N}_\tau,\tau,\Delta\tau)=\frac{1}{\Delta\tau}\sum_{\mathcal{N}_{\tau+\Delta\tau}}[\Delta_\tau\mathcal{N}_\tau(n)]^k\Delta p, \tag{A1}$$

where $\Delta_\tau\mathcal{N}_\tau(n)=\mathcal{N}_{\tau+\Delta\tau}(n)-\mathcal{N}_\tau(n)$ and Δp is the error of the conditional probability, namely

$$\Delta p=\frac{\Delta p_{joint}}{p(\mathcal{N}_\tau,\tau)}+\frac{p(\mathcal{N}_{\tau+\Delta\tau},\tau+\Delta\tau;\mathcal{N}_\tau,\tau)\Delta p_{ref}}{[p(\mathcal{N}_\tau,\tau)]^2}, \tag{A2}$$

with Δp_{joint} and Δp_{ref} representing, respectively, the errors of the joint PDF $p(\mathcal{N}_{\tau+\Delta\tau},\tau+\Delta\tau;\mathcal{N}_\tau,\tau)$ and of the PDF $p(\mathcal{N}_\tau,\tau)$ of the reference time. These two errors are extracted directly from the simulation as the square root of the number of values inside each corresponding bin.

The error function for the drift and diffusion coefficients in Fig. 4 are obtained directly from a linear regression of the corresponding conditional moments as functions of $\Delta\tau$, where the error function in Eq. (A1) for the conditional moment is used as input. A similar error analysis was used for the coefficients in the two-dimensional case (Fig. 6).

The parametrizations in Eqs. (6) and (7), in Table I and in Eqs. (22) were performed using standard least-square procedures [23].

APPENDIX B: INTEGRATING THE FOKKER-PLANCK EQUATION

We introduce the parametrizations (6) and (7) into the Fokker-Planck equation

$$\frac{\partial}{\partial\tau}p(\mathcal{N}_\tau,\tau|\mathcal{N}_{\tau'},\tau')=\mathcal{L}_{FP}p(\mathcal{N}_\tau,\tau|\mathcal{N}_{\tau'},\tau'), \tag{B1}$$

where $\mathcal{L}_{FP}$ is the operator

$$\mathcal{L}_{FP}=\left(-\frac{\partial}{\partial\mathcal{N}_\tau}D^{(1)}(\mathcal{N}_\tau,\tau)+\frac{\partial^2}{\partial\mathcal{N}_\tau^2}D^{(2)}(\mathcal{N}_\tau,\tau)\right). \tag{B2}$$

The initial condition $p(\mathcal{N}_0,\tau_0)$ is taken at $t_0=t_{ref}=32$ and the integration is carried out by means of a suitable discretization scheme [21] yielding

$$p(\mathcal{N}_{\tau+\Delta\tau},\tau+\Delta\tau|\mathcal{N}_\tau,\tau)=\frac{1}{2\sqrt{\pi D^{(2)}(\mathcal{N}_\tau,\tau)\Delta\tau}}\times\exp\left(-\frac{(\mathcal{N}_{\tau+\Delta\tau}-\mathcal{N}_\tau-D^{(1)}(\mathcal{N}_\tau,\tau)\Delta\tau)^2}{4D^{(2)}(\mathcal{N}_\tau,\tau)\Delta\tau}\right). \tag{B3}$$

The Fokker-Planck Eq. (B1) describes the evolution of *conditional* PDFs. To know at each time τ the single PDF $p(\mathcal{N}_{\tau+\Delta\tau},\tau+\Delta\tau)$, as the ones shown in Fig. 5 for time-steps $\Delta\tau=1$, 2, 3, 4 and 5, one must integrate at each time step the conditional PDF multiplied by the previous single PDF. This is done by using the Chapman-Kolmogorov equation

$$p(\mathcal{N}_{\tau+\Delta\tau},\tau+\Delta\tau)=\int p(\mathcal{N}_{\tau+\Delta\tau},\tau+\Delta\tau|\mathcal{N}_\tau,\tau)p(\mathcal{N}_\tau,\tau)d\mathcal{N}_\tau. \tag{B4}$$

APPENDIX C: DRIFT AND DIFFUSION COEFFICIENTS IN TWO-DIMENSIONS

For the two-dimensional case of two coupled Langevin equations, Eqs. (9), the Kramers-Moyal coefficients read [21]

$$D_i^{(1)}(P_1,P_2,\tau)=\lim_{\Delta\tau\to0}M_i^{(1)}(P_1,P_2,\tau,\Delta\tau), \tag{C1a}$$

$$D_{ij}^{(2)}(P_1,P_2,\tau)=\tfrac{1}{2}\lim_{\Delta\tau\to0}M_{ij}^{(2)}(P_1,P_2,\tau,\Delta\tau), \tag{C1b}$$

where $i,j=1,2$ and conditional moments are given by

$$M_i^{(1)}(P_1,P_2,\tau,\Delta\tau)\simeq\frac{1}{\Delta\tau}\sum_{P_i'}\Delta P_i p, \tag{C2a}$$

$$M_{ij}^{(2)}(P_1,P_2,\tau,\Delta\tau)\simeq\frac{1}{\Delta\tau}\sum_{P_i',P_j'}\Delta P_i\Delta P_j p, \tag{C2b}$$

where $\Delta P_i = P'_i(\tau+\Delta\tau) - P_i(\tau)$ and where now the sum is over the bins discretization, namely the PDF of $P'_{i,j}(\tau+\Delta\tau)$, and $p \equiv p[\vec{P}'(\tau+\Delta\tau), \tau+\Delta\tau | \vec{P}(\tau), \tau]$ is the conditional probability of observing the two values $\vec{P}' = (P'_1, P'_2)$ at $\tau+\Delta\tau$ knowing that the values $\vec{P} = (P_1, P_2)$ were observed at τ. As one clearly sees from Eq. (C2b) the matrix of second order conditional moments and consequently $D^{(2)}$ are symmetric, $D^{(2)}_{12} = D^{(2)}_{21}$.

[1] P. D. Jones, T. J. Osborn, and K. R. Briffa, Science **292**, 662 (2001).
[2] K. Higuchi, J. Huang, and A. Shabbar, Int. J. Climatol. **19**, 1119 (1999).
[3] H. Paeth, M. Latif, and A. Hense, Clim. Dyn. **21**, 63 (2003).
[4] C. Appenzeller, T. F. Stocker, and M. Anklin, Science **282**, 446 (1998).
[5] C. Wunsch, Bull. Am. Meteorol. Soc. **80**, 245 (1999).
[6] S. Jevrejeva, J. C. Moore, and A. Grinsted, J. Geophys. Res. **108**, 4677 (2003).
[7] J. L. Melice and J. Servain, Clim. Dyn. **20**, 447 (2003).
[8] H. Wanner, S. Bronnimann, C. Casty, D. Gyalistras, J. Luterbacher, C. Schmutz, D. B. Stephenson, and E. Xoplaki, Surv. Geophys. **22**, 321 (2001).
[9] J. Hurrel, Science **279**, 676 (1995).
[10] O. A. Lucero and N. C. Rodriguez, Int. J. Climatol. **22**, 805 (2002).
[11] Data are available at http://www.cru.uea.ac.uk/cru/data/nao.htm.
[12] D. B. Stephenson, V. Pavan, and R. Bojariu, Int. J. Climatol. **20**, 1 (2000).
[13] C. Collette and M. Ausloos, Int. J. Mod. Phys. C **15**, 1353 (2004).
[14] Ch. Renner, J. Peinke, and R. Friedrich, J. Fluid Mech. **433**, 383 (2001).
[15] J. Gradisek, S. Siegert, R. Friedrich, and I. Grabec, Phys. Rev. E **62**, 3146 (2000).
[16] R. Friedrich, J. Peinke, and Ch. Renner, Phys. Rev. Lett. **84**, 5224 (2000).
[17] M. Waechter, F. Riess, Th. Schimmel, U. Wendt, and J. Peinke, Eur. Phys. J. B **41**, 259 (2004).
[18] K. Ivanova and M. Ausloos, J. Geophys. Res. **107**, 4708 (2002).
[19] P. Sura, J. Atmos. Sci. **60**, 654 (2003).
[20] R. Friedrich and J. Peinke, Phys. Rev. Lett. **78**, 863 (1997).
[21] H. Risken, *The Fokker Planck Equation* (Springer, Berlin, 1984).
[22] H. D. I. Abarbanel, R. Brown, J. J. Sidorowich, and L. S. Tsimring, Rev. Mod. Phys. **65**, 1331 (1993).
[23] W. H. Press, B. P. Flannery, S. A. Teukolsky, and W. T. Vetterling, *Numerical Recipes* (Cambridge University Press, Cambridge, 1992).
[24] T. Jónsson and M. Miles, Geophys. Res. Lett. **28**, 4231 (2001).
[25] B. Epstein, *Partial Differential Equations* (McGraw-Hill, New York, 1962).
[26] M. Siefert, A. Kittel, R. Friedrich, and J. Peinke, Europhys. Lett. **61**, 466 (2003).
[27] P. G. Lind, A. Mora, J. A. C. Gallas, and M. Haase (unpublished).